Dependence of Alamethicin Membrane Orientation on the Solution Concentration

Pei Yang, **Fu-Gen Wu**, and **Zhan Chen**[*]
Department of Chemistry, 930 North University Avenue, University of Michigan, Ann Arbor, Michigan 48109

Abstract

Alamethicin has been extensively studied as an antimicrobial peptide and is widely used as a simple model for ion channel proteins. It has been shown that the antimicrobial activity of peptides is related to their membrane orientation. In this study, we determined the relationship between the solution concentration of alamethicin and its membrane orientation in lipid bilayers using sum frequency generation (SFG) vibrational spectroscopy. Our SFG results indicated that the alamethicin molecules more or less lay down on the surface of 1-palmitoyl-2-oleoyl-sn-glycero-3-phosphocholine (POPC) lipid bilayers at a low peptide concentration of 0.84 μM; the α-helix segment tilts at about 88°, and 3_{10}-helix segment tilts at about 58° versus the surface normal. However, when the peptide concentration was increased to 15.6 μM, we observed that alamethicin molecules further inserted into the lipid bilayers: the α-helical component changes its orientation to make a 37° tilt from the lipid bilayer normal, and the 3_{10}-helical component tilts at about 50° versus the surface normal. This is in agreement with the barrel-stave mode for the alamethicin–cell membrane interaction as reported previously. Additionally, we have also studied membrane orientation of alamethicin as a function of peptide concentration with SFG. Our results showed that the membrane orientation of the alamethicin α-helical component changed substantially with the increase of the alamethicin concentration, while the membrane orientation of the 3_{10}-helical component remained more or less the same.

Keywords

Sum frequency generation vibrational spectroscopy; antimicrobial peptide; supported lipid bilayer; α-helix; 3_{10}-helix

1. Introduction

Antimicrobial peptides have been extensively studied in the recent years, which interact with the cell membranes to overcome bacteria drug resistance.[1–4] Alamethicin is a 20-residue hydrophobic antimicrobial peptide extracted from the fungus *Trichoderma viride* that forms voltage-gated ion channels in cell membranes.[5–9] It has been extensively studied as an antimicrobial peptide and also used frequently as a model for larger channel proteins and for studying of ion channel gating mechanisms.[10–13] Ion channels represent an important class of transmembrane proteins that regulate ionic permeability in cell membranes.[14–19] They are key elements in cell signaling, electrical excitability, and fluid transport, and are validated drug targets for diseases such as heart disease, diabetes and Parkinson's disease.[20–26]

[*]To whom correspondence should be addressed. Fax: 734-647-4865. zhanc@umich.edu..

The action mechanisms of alamethicin in cell membranes have been widely studied. It is currently believed that alamethicin interacts with cell membranes through the barrel-stave mode, in which the molecules form parallel bundles of the helical monomers surrounding the central, water-filled pore.[6] Recently, our group applied sum frequency generation vibrational spectroscopy (SFG) to investigate the molecular interactions between alamethicin and different lipid bilayers with and without the presence of a membrane potential.[27,28] SFG is a nonlinear optical spectroscopic technique that provides vibrational spectra of surfaces and interfaces with a submonolayer surface specificity.[29–40] It requires only a very small amount of samples, and can probe surfaces and interfaces in real-time *in situ*.[41–54]

An alamethicin molecule contains an α-helical structure (residues 1–13) and a 3_{10}-helix (residues 14–20). It has been shown that these two different secondary structures generate SFG amide I signals with different peak centers.[27] Therefore, we can determine the membrane orientation for each component in alamethicin using polarized SFG spectra. Our previous studies indicated that in the absence of a membrane potential, alamethicin molecules can insert into fluid-phase lipid bilayers, but lie down and/or aggregate on gel-phase bilayer surfaces.[27] Our results also showed that the change in the pH of the peptide solution can modulate the membrane potential, inducing a decrease in both the tilt and bend angles of the two helices in alamethicin.[28]

Additionally, it is important to study the alamethicin–membrane interactions at different peptide concentrations. The orientation of alamethicin in different concentrations on lipid bilayers is related to its gating mechanisms and antimicrobial functions, which have not been fully understood.[13,14] Contradictory orientations of alamethicin in cell membranes in the absence of membrane potential have been reported. Alamethicin has been suggested to adopt a transmembrane orientation,[10–12, 15–19] lie down on the membrane surface,[20–22] or both.[23.24] Such different orientations may depend on peptide concentrations.

In this paper, we will report SFG experimental results for alamethicin interacting with model cell membranes at different peptide concentrations. Alamethicin strongly interacts with phosphatidylcholine (PC) and phosphatidylglycerol (PG) fluid phase lipids, but not PC and PG gel phase lipids.[27] Therefore this study chooses 1-palmitoyl-2-pleoyl-sn-glycero-3-phosphocholine (POPC), a lipid in its fluid phase at room temperature, to study the concentration effect of the peptide. Our results indicate that alamethicin molecules change membrane orientations as a function of peptide concentrations. They lie down on the model cell membrane surface at low peptide concentrations and can insert into lipid bilayers at higher concentrations. The orientation angle of the α-helical segment changed substantially after increasing the alamethicin concentration, while the orientation angle of the 3_{10}-helical segment only changed slightly. We also followed the real-time molecular reorientation process of alamethicin during the initial interaction with the model cell membranes.

2. Materials and Methods

2.1. Materials

Alamethicin from *Trichoderma viride* was purchased from Sigma-Aldrich (St. Louis, MO) with a minimum purity of 90%. The POPC lipid was purchased from Avanti Polar Lipids (Alabaster, AL), and its molecular structure was shown in scheme 1. Right-angle CaF_2 prisms were purchased from Altos (Trabuco Canyon, CA). The CaF_2 prisms were thoroughly cleaned using a procedure with following steps: They were soaked in toluene for 24 hours and then in Contrex AP solution from Decon Laboratories (King of Prussia, PA) for 30 minutes. After that, they were cleaned in methanol for 10 minutes and then rinsed thoroughly with deionized (DI) water. The prisms were treated in a glow discharge plasma

chamber for 4 minutes immediately before the lipid deposition. Substrates were tested using SFG, and no signal from contamination was detected. Single lipid bilayers were prepared on CaF$_2$ substrates using the Langmuir-Blodgett and Langmuir-Schaefer (LB/LS) method. A KSV2000 LB system and ultrapure water from Millipore system (Millipore, Bedford, MA) were used throughout the experiments for bilayer preparation, as described previously.[43] All of the experiments were carried out at room temperature (~24°C), at which the POPC/POPC bilayers are in the fluid phase. For alamethicin–lipid bilayer interaction experiments, an appropriate amount of alamethicin solution (in methanol with a concentration of 2.5 mg/mL) was injected into the reservoir filled with 1.6 mL of ultrapure water (in contact with the supported lipid bilayer) to achieve the desired peptide solution concentration. The SFG spectra were then collected after the alamethicin–lipid bilayer interaction reached equilibrium and SFG signal became stable (around 1 hour after the injection of the alamethicin solution into the subphase of the lipid bilayer). A magnetic micro stirrer was used to ensure a homogeneous concentration of alamethicin in the subphase below the lipid bilayer.

2.2. SFG

SFG is a second-order nonlinear optical spectroscopic technique that has submonolayer surface sensitivity.[55–70] This surface sensitivity makes SFG an ideal technique to monitor the reorientation process of submonolayer molecules *in situ*. The details regarding SFG theories and measurements have been published previously,[71–84] and will not be repeated here. In our experiments, two laser beams (a 532 nm visible and a frequency tunable infrared) are overlapped in space and time on the sample, generating a signal at the sum frequency ($\omega_{vis}+\omega_{ir}=\omega_{sum}$). The pulse energies of both input beams are approximately 100 μJ, and the beam sizes are approximately 500 μm. SFG spectra from interfacial alamethicin in different polarization combinations including ssp (s-polarized output SFG signal, s-polarized input visible beam, and p-polarized input IR beam) and ppp were collected using the near total internal reflection geometry. The average orientation of a peptide secondary structure can be deduced by analyzing the polarized ssp and ppp SFG amide I signal (between 1600 and 1700 cm^{-1}).

2.3. Orientation Analysis

In our previous studies, we showed that SFG spectra collected from alamethicin at interfaces contain two peaks.[27,28] The 1671 cm^{-1} signal is contributed by the alamethicin α-helical component, and the signal centered at 1638 cm^{-1} is generated by the 3$_{10}$-helical structure. The peptide orientation information can be obtained by relating the SFG nonlinear optical susceptibility tensor element χ_{ijk}(*i, j, k = x, y, z*) to the SFG molecular hyperpolarizability tensor element β_{lmn}(*l, m, n = a, b, c*). We have developed orientation analysis methods to determine orientation angles of α-helical and 3$_{10}$-helical structures by using SFG amide I spectra collected with ssp and ppp polarization combinations. Such details have been introduced in our previous papers and will not be repeated here.[45,46] The orientation analysis method has been successfully applied to examine the membrane orientation of peptides and proteins such as alamethicin,[27,28] magainin 2,[46] cecropin P1,[42] MSI-78,[43] Pep-1,[47] melittin,[48] cytochrome b5,[49] and G-proteins.[44,50]

3. Results and Discussion

3.1 Orientation of Alamethicin in a POPC/POPC Bilayer

After the alamethicin stock solution was injected into the subphase of a POPC/POPC bilayer, the SFG signal at 1671 cm^{-1} was detected and then monitored as a function of time. The SFG signal intensity at 1671 cm^{-1} increased gradually and became stable at about one hour after the introduction of alamethicin solution to the subphase. The ppp and ssp

polarized SFG spectra of alamethicin in a POPC/POPC bilayer were collected. Figure 1 shows the SFG spectra collected at about one hour after a 0.84 μM (top) or 15.6 μM (bottom) alamethicin solution was injected into the subphase in contact with the POPC/POPC bilayer.

At a lower alamethicin concentration of 0.3 μM, no discernible SFG amide I signal from alamethicin in the lipid bilayer could be detected (data not shown). This can be explained by the fact that the interaction between alamethicin molecules and POPC/POPC bilayer could be very weak at this low peptide concentration. Not enough alamethicin molecules segregate to the lipid bilayer surface and thus no SFG signal can be detected. At the peptide concentration of 0.84 μM, we observed three peaks in the SFG spectra: a dominant peak centered at 1671 cm^{-1}, originated from the alamethicin α-helical structure, a 1638 cm^{-1} peak contributed by the 3_{10}-helix, and a 1705 cm^{-1} signal generated by the carbonyl group of the lipid bilayer.[28] The solid lines in Figure 1 are the fitting results, and the corresponding fitting parameters are listed in Table 1. The details of the SFG peak fitting methods have been described in previous publications and will not be reiterated here.[46] According to the fitting results, we obtained the measured SFG ppp and ssp signal strength ratio (or χ_{ppp}/χ_{ssp}) of 2.29 for 0.84 μM and 1.80 for 15.6 μM at 1671 cm^{-1}, and 2.04 for 0.84 μM and 1.77 for 15.6 μM at 1638 cm^{-1}. By using these ratios, we can determine the orientation angles of different secondary structures of alamethicin in the POPC/POPC bilayers at different peptide concentrations.

Alamethicin consists of two helical segments due to the presence of the helix-breaking Pro 14 residue. According to the previous publications,[27,28] the α-helical structure which contains residues 1–13 contributes to the signal at 1671 cm^{-1}; the 3_{10}-helical structure formed by residues 14–20 contributes to the signal at 1638 cm^{-1}. Here, we define that the orientation angle θ_1 represents the tilt angle between the principal axis of the α-helical structure (with residues 1–13) and the POPC/POPC bilayer surface normal, while angle θ_2 represents the tilt angle between the principal axis of the 3_{10}-helix (with residues 14–20) and the POPC/POPC bilayer surface normal. The definition of the tilt angles of alamethicin in POPC/POPC bilayer is shown in Figure 2.

Using the relation between the measured χ_{ppp}/χ_{ssp} ratio for the peak at 1671 cm^{-1} and the α-helical orientation angle θ_1 for α-helix with thirteen amino acids, the orientation angle can be deduced assuming a δ-orientation distribution (Figure 3). The experimentally measured χ_{ppp}/χ_{ssp} ratio for the peak at 1671 cm^{-1} is 2.29 for 0.84 μM and 1.80 for 15.6 μM, yielding an orientation angle (θ_1) of 88° for 0.84 μM and 37° for 15.6 μM.

The relation between the measured χ_{ppp}/χ_{ssp} ratio at 1638 cm^{-1} and the 3_{10}-helix orientation angle θ_2 for a 3_{10}-helix with seven amino acids can be deduced using the developed method assuming a δ-orientation distribution (Figure 4).[45] The orientation angle (θ_2) was deduced to be 58° for 0.84 μM and 50° for 15.6 μM.

Experiments with 3.6 μM and 10.8 μM alamethicin were also performed. SFG amide I spectra were collected as described above (not shown). The spectra were fitted and peptide orientations were deduced.

Table 2 shows the orientation angles of alamethicin α-helical (θ_1) and 3_{10}-helical (θ_2) segments associated with the POPC/POPC bilayer at four different peptide concentrations. As shown in Table 2, after the peptide concentration was increased, the tilt angle θ_1 decreased substantially, indicating that the orientation of the α-helical segment in alamethicin changed from "surface lying down orientation" to "transmembrane orientation" in the POPC/POPC bilayer. At a concentration of 0.84 μM, the α-helical segment (θ_1) adopts a tilt angle of 88° from the bilayer normal; almost completely lying down on the lipid

bilayer. At a peptide concentration of 3.6 µM, the orientation angle decreased from 88° to 59°. When the peptide concentration further increased to 10.8 µM, the orientation angle decreased to 46°. As the concentration increased to 15.6 µM, the orientation angle of α-helical segment in alamethicin was determined to be approximately 37° relative to the bilayer normal, similar to a transmembrane orientation. This shows that the increase in peptide concentration induces the α-helical segment in alamethicin to change orientation from the "perpendicular to the POPC/POPC bilayer normal or lying down orientation" to the "parallel to the bilayer normal or standing up orientation". However, the tilt angle of 3_{10}-helix (θ_2) only decreased slightly, from 58° to 50° when the peptide concentration increased from 0.84 µM to 15.6 µM. This indicates that the orientation angle of 3_{10}-helix remains almost the same at different peptide concentrations.

Figure 5 shows schematics of membrane orientations of alamethicin at the solution concentrations of 0.84 µM (top) and 15.6 µM (bottom). At the low concentration of 0.84 µM, the α-helical segment is oriented on the bilayer surface with a tilt angle of 88°, while the 3_{10}-helix is oriented on the bilayer surface with an angle of 58°. In this situation, the alamethicin molecule lies down on the POPC/POPC bilayer. Because the 3_{10}-helix is hydrophilic,[22] we believe that it oriented outside of the hydrophobic core of the lipid bilayer at a low peptide concentration. At the high alamethicin concentration of 15.6 µM, the α-helical segment inserts into the lipid bilayer at an angle of 37°, the 3_{10}-helix is oriented at an angle of 50°. The entire alamethicin molecule inserts into the lipid bilayer.

Our results showed that the alamethicin molecules lie down on the lipid bilayer surface at low peptide concentrations, while they stand up on the bilayer surface at high peptide concentrations. The oriented circular dichroism (OCD) experimental results indicated that the axes of the helical peptides are oriented parallel to the plane of the membrane at low peptide concentrations and are perpendicular to the plane of the bilayer at high peptide concentrations,[25,26] which agree with our SFG results. It was believed that while at low peptide concentrations the energy level of the peptide surface adsorption state is lower than that of the peptide pore forming state. At high peptide concentrations, the former eventually exceeds the latter and, hence, the transition from peptide lying down to membrane insertion at a high peptide concentration occurs.[25] That is to say, at different peptide concentrations, the membrane–peptide interactions are different. The molecular details should be further investigated in the future. It was also concluded that the alamethicin α-helix segment is more hydrophobic and 3_{10}-helix segment is more hydrophilic,[22] so the α-helical segment prefers to insert into the lipid bilayer while the hydrophilic 3_{10}-helix should be oriented outside of the hydrophobic core of the lipid bilayer at high peptide concentrations (Figure 5).

Our previous studies on interactions between helical peptides and lipid bilayers including MSI-78,[43] cecropin P1,[42] and melittin[48] indicated that at high peptide concentrations, the SFG data cannot be interpreted using a single orientation distribution. It was believed that multiple orientations of peptides associated with lipid bilayers exist, which is due to the toroidal mode of action. In the toroidal mode, the peptides can have varied orientations while forming transmembrane pores. Here, a single orientation angle distribution can satisfy the observed SFG data for the entire peptide concentration range investigated. Therefore, we believe that this is due to the barrel-stave mode of action, in which all the peptides more or less stand up in the membrane.

It was shown that the orientation of the alamethicin (which dependent on the peptide/lipid ratio) is related to its activity.[23,26] However, in those studies, samples were prepared differently and peptides were mixed with lipids directly. While in this work, we use planar supported lipid bilayer system and injected peptide solutions with different concentrations into subphase. Therefore it is difficult to correlate our results to those data. Our experiments

are more closely related to the physiologically relevant conditions. To summarize, we reveal the relationship between alamethicin concentration and the alamethicin orientation, and point out the concentration-dependent change of the peptide from its inactive state of lying down on lipid bilayer to the active state of forming transmembrane pores.

3.2. Binding process of alamethicin with the POPC/POPC lipid bilayer

We also followed the kinetics of the alamethicin-POPC/POPC bilayer association at different peptide concentrations. Such kinetics can be monitored by detecting the SFG amide I signal intensity change as a function of time.

Figure 6 shows the time-dependent SFG ssp spectral intensity changes at 1671 cm^{-1} (from the α-helix structure) at 0.84 μM (top) and 15.6 μM (bottom) peptide solution concentrations. The alamethicin stock solution was injected at 200 s into the lipid subphase. For both of low and high concentrations, the SFG intensity at 1671 cm^{-1} increased sharply at first, followed by a decrease and another increase. It is well known that the SFG signal depends on both the number density of signal-generating functional groups and the orientation of such functional groups.

When the peptide molecules were injected into the subphase at 200 s, the alamethicin solution concentration in the subphase is much higher than the peptide concentration associated with the lipid bilayer. Due to diffusion, the number of alamethicin molecules bound to the POPC/POPC bilayer should increase until equilibrium is reached. The increase should be monotonic as a function of time. The final alamethicin surface coverage on the lipid bilayer is related to the peptide concentration in subphase. If the alamethicin molecules always adopt a similar orientation on the lipid bilayer during the whole binding process, the SFG intensity should increase monotonically as a function of time, and finally become stable. But we observed that the SFG intensity dropped around 350 s in our experiment. As mentioned previously, SFG intensity changes can be a result of either the change of number density of the peptide on the membrane, or the reorientation of the peptide secondary structures, or a combination of both. We believe that the SFG intensity decrease at 350 s may be due to the reorientation of the lipid bilayer associated alamethicin molecules. Based on our calculation, the helical peptides have the maximum ssp SFG amide I signal intensity when they stand up at the interface and have the minimum ssp SFG amide I signal intensity when they lie down on the surface. Perhaps, the lipid bilayer associated alamethicin molecules initially stand up, then some of these peptide molecules changed orientation and tilted more towards the surface. Therefore, the SFG intensity decreased even when more peptide molecules were associated with the lipid bilayer. This orientation change process is fast, and takes about ~100 s. The SFG amide I signal intensity increased again at ~500 s because more alamethicin molecules became associated with the POPC/POPC bilayer and no further orientation change occurred.

At the low peptide concentration of 0.84 μM, the ssp SFG amide I signal intensity from alamethicin in the lipid bilayer no longer increased after 4000 s. However, at a high peptide concentration of 15.6 μM, the SFG amide I signal intensity reached a plateau at 2000 s. This indicates that alamethicin needs less time to reach equilibrium to associate with the POPC/POPC bilayer when the peptide concentration is higher.

4. Conclusion

It was found that the alamethicin molecules adopt varied orientations in model cell membranes (POPC/POPC bilayers) at different peptide concentrations. They lie down on the lipid bilayer surface at a low peptide concentration of 0.84 μM: The α-helical segment orients at about 88° versus the surface normal, while the 3$_{10}$-helical segment tilts at about

58° versus the surface normal. When the peptide concentration increases, the alamethicin molecules can insert into the lipid bilayer and change the membrane orientation. When the peptide concentration reaches 15.6 μM, alamethicin molecules insert into the lipid bilayers: The α-helix tilts at about 37° versus the surface normal, and the 3_{10}-helix tilts at about 50° versus the surface normal. It is interesting to observe that over this entire peptide concentration range, the orientation angle of the α-helical segment changed substantially, while the orientation of the 3_{10}-helical structure only changed slightly. Also, the observed SFG data can be interpreted by a single orientation distribution over the peptide concentration range investigated, indicating the barrel-stave mode of action.

Acknowledgments

References

1. Zasloff M. Antimicrobial Peptides of Multicellular Organisms. Nature. 2002; 415:389–395. [PubMed: 11807545]

2. Giuliani A, Pirri G, Nicoletto SF. Antimicrobial Peptides: An Overview of a Promising Class of Therapeutics. Cent. Eur. J. Biol. 2007; 2:1–33.

3. Dhople V, Krukemeyer A, Ramamoorthy A. The Human Beta-defensin-3, An Antibacterial Peptide with Multiple Biological Functions. Biochim. Biophys. Acta. 2006; 1758:1499–1512. [PubMed: 16978580]

4. Epand RF, Maloy L, Ramamoorthy A, Epand RM. Amphipathic Helical Cationic Antimicrobial Peptides Promote Rapid Formation of Crystalline States in the Presence of Phosphatidylglycerol: Lipid Clustering in Anionic Membranes. Biophys. J. 2010; 98:2564–2573. [PubMed: 20513400]

5. Woollet GA, Wallace BA. Model Ion Channels: Gramicidin and Alamethicin. J. Member. Biol. 1992; 129:109–136.

6. Archer SJ, Ellena JF, Cafiso DS. Dynamics and Aggregation of the Peptide Ion Channel Alamethicin. Biophys. J. 1991; 60:389–398. [PubMed: 1717016]

7. Cafiso DS. ALAMETHICIN: A Peptide Model for Voltage Gating and Protein-Membrane Interactions. Annu. Rev. Biophys. Biomol. Struct. 1994; 23:141–165. [PubMed: 7522664]

8. Bechinger B. Structure and Functions of Channel-Forming Peptides: Magainins, Cecropins, Melittin and Alamethicin. J. Membr. Biol. 1997; 156:197–211. [PubMed: 9096062]

9. Fox RO, Richards FM. A Voltage-gated ion Channel Model Inferred from the Crystal Structure of Alamethicin at 1.5-A Resolution. Nature. 1982; 200:325–330. [PubMed: 6292726]

10. North CL, Barranger-Mathys M, Cafiso DS. Membrane Orientation of the N-terminal Segment of Alamethicin Determined by Solid-State 15N NMR. Biophys. J. 1995; 69:2392–2397. [PubMed: 8599645]

11. Bak M, Baywater RP, Hohwy M, Thomsen JK, Adelhorst K, Jackobsen HJ, Sorensen OW, Nielsen NC. Conformation of Alamethicin in Oriented Phospholipid Bilayers Determined by 15N Solid-State Nuclear Magnetic Resonance. Biophys. J. 2001; 81:1684–1698. [PubMed: 11509381]

12. Salnikov ES, Friedrich H, Li X, Bertani P, Reissmann S, Hertweck C, O'Neil JDJ, Raap J, Bechinger B. Structure and Alignment of the Membrane-Associated Peptaibols Ampullosporin A and Alamethicin by Oriented 15N and 31P Solid-State NMR Spectroscopy. Biophys. J. 2009; 96:86–100. [PubMed: 18835909]

13. Milov AD, Samoilova RI, Tsvetkov YD, Zotti MD, Toniolo C, Raap J. PELDOR Conformational Analysis of bis-Labeled Alamethicin Aggregated in Phospholipid Vesicles. J. Phys. Chem. B. 2008; 112:13469–13472. [PubMed: 18837536]

14. Stella L, Burattini M, Mazzuca C, Palleschi A, Venanzi M, Coin I, Peggion C, Toniolo C, Pispisa B. Alamethicin Interaction with Lipid Membranes: A Spectroscopic Study on Synthetic Analogues. Chem. Biodiversity. 2007; 4:1299–1312.

15. Kessel A, Cafiso DS, Ben-Tal N. Continuum Solvent Model Calculations of Alamethicin-Membrane Interactions: Thermodynamic Aspects. Biophys. J. 2000; 78:571–583. [PubMed: 10653772]

16. Marsh D, Jost M, Peggion C, Toniolo C. TOAC Spin Labels in the Backbone of Alamethicin: EPR Studies in Lipid Membranes. Biophys. J. 2007; 92:473–481. [PubMed: 17056731]

17. Marsh D, Jost M, Peggion C, Toniolo C. Lipid Chain-Length Dependence for Incorporation of Alamethicin in Membranes: Electron Paramagnetic Resonance Studies on TOAC-Spin Labeled Analogs. Biophys. J. 2007; 92:4002–4011. [PubMed: 17351010]

18. Marsh D. Orientation and Peptide-Lipid Interactions of Alamethicin Incorporated in Phospholipid Membranes: Polarized Infrared and Spin-Label EPR Spectroscopy. Biochemistry. 2009; 48:729–737. [PubMed: 19133787]

19. Salnikoy ES, Zotti MD, Formaggio F, Li X, Toniolo C, O'Neil JDJ, Raap J, Dzuba SA, Bechinger B. Alamethicin Topology in Phospholipid Membranes by Oriented Solid-state NMR and EPR Spectroscopies: a Comparison. J. Phys. Chem. B. 2009; 113:3034–3042. [PubMed: 19708263]

20. Sansom MSP. Structure and Function of Channel-forming Peptaibols. Q. Rev. Biophys. 1993; 26:365–421. [PubMed: 7520180]

21. Ionov R, El-Abed A, Angelova A, Goldmann M, Peretti P. Asymmetrical Ion-Channel Model Inferred from Two-Dimensional Crystallization of a Peptide Antibiotic. Biophys. J. 2000; 78:3026–3035. [PubMed: 10827981]

22. Mottamal M, Lazaridis T. Voltage-dependent Energetics of Alamethicin Monomers in the Membrane. Biophys. Chem. 2006; 122:50–57. [PubMed: 16542770]

23. Chen FY, lee MT, Huang HW. Sigmoidal Concentration Dependence of Antimicrobial Peptide Activities: A Case Study on Alamethicin. Biophys. J. 2002; 82:908–914. [PubMed: 11806932]

24. Huang HW, Wu Y. Lipid-alamethicin Interactions Influence Alamethicin Orientation. Biophys. J. 1991; 60:1079–1087. [PubMed: 19431805]

25. Huang HW. Action of Antimicrobial Peptides: Two-State Model. Biochemistry. 2000; 39:8347–8352. [PubMed: 10913240]

26. Huang HW. Molecular Mechanism of Antimicrobial Peptides: The Origin of Cooperativity. Biochim. Biophys. Acta. 2006; 1758:1292–1302. [PubMed: 16542637]

27. Ye S, Nguyen K, Chen Z. Interactions of Alamethicin with Model Cell Membranes Investigated Using Sum Frequency Generation Vibrational Spectroscopy in Real Time in Situ. J. Phys. Chem. B. 2010; 114:3334–3340. [PubMed: 20163089]

28. Ye S, Li H, Wei F, Jasensky J, Boughton AP, Yang P, Chen Z. Observing a Model Ion Channel Gating Action in Model Cell Membranes in Real Time in Situ: Membrane Potential Change Induced Alamethicin Orientation Change. J. Am. Chem. Soc. 2012; 134:6237–6243. [PubMed: 22420296]

29. Eisenthal KB. Liquid Interfaces Probed by Second-Harmonic and Sum-Frequency Spectroscopy. Chem. Rev. 1996; 96:1343–1360. [PubMed: 11848793]

30. Richmond GL. Molecular Bonding and Interactions at Aqueous Surfaces as Probed by Vibrational Sum Frequency Spectroscopy. Chem. Rev. 2002; 102:2693–2724. [PubMed: 12175265]

31. Scatena LF, Brown MG, Richmond GL. Water at Hydrophobic Surfaces: Weak Hydrogen Bonding and Strong Orientation Effects. Science. 2001; 292:908–912. [PubMed: 11340199]

32. Bain CD. Sum-frequency Vibrational Spectroscopy of the Solid/Liquid Interface. J. Chem. Soc., Dalton Trans. 1995; 91:1281–1296.

33. Shen YR. A Few Selected Applications of Surface Nonlinear Optical Spectroscopy. Proc. Natl. Acad. Sci. U.S.A. 1996; 93:12104–12111. [PubMed: 8901540]

34. Zhuang X, Miranda PB, Kim D, Shen YR. Mapping Molecular Orientation and Conformation at Interfaces by Surface Nonlinear Optics. Phys. Rev. B. 1999; 59:12632–12640.

35. Chen Z, Shen YR, Somorjai GA. Studies of Polymer Surfaces by Sum Frequency Generation Vibrational Spectroscopy. Annu. Rev. Phys. Chem. 2002; 53:437–465. [PubMed: 11972015]

36. Chen P, Kung KY, Shen YR, Somorjai GA. Sum Frequency Generation Spectroscopic Study of CO/Ethylene Coadsorption on the Pt(111) Surface and CO Poisoning of Catalytic Ethylene Hydrogenation. Surf. Sci. 2001; 494:289–297.

37. Kim J, Somorjai GA. Molecular Packing of Lysozyme, Fibrinogen, and Bovine Serum Albumin on Hydrophilic and Hydrophobic Surfaces Studied by Infrared–Visible Sum Frequency Generation and Fluorescence Microscopy. J. Am. Chem. Soc. 2003; 125:3150–3158. [PubMed: 12617683]

38. Kim J, Cremer PS. Elucidating Changes in Interfacial Water Structure upon Protein Adsorption. Chem. Phys. Chem. 2001; 2:543–546.

39. Kim G, Gurua MC, Lim SM, Cremer PS. Investigations of the Orientation of a Membrane Peptide by Sum Frequency Spectroscopy. J. Phys. Chem. B. 2003; 107:1403–1409.

40. Wang H, Gang W, Lu R, Rao Y, Wu B. Quantitative Spectral and Orientational Analysis in Surface Sum Frequency Generation Vibrational Spectroscopy (SFG-VS). Int. Rev. Phys. Chem. 2005; 24:191–256.

41. Thennarasu S, Huang R, Lee DK, Yang P, Maloy L, Chen Z, Ramamoorthy A. Limiting an Antimicrobial Peptide to the Lipid-Water Interface Enhances Its Bacterial Membrane Selectivity: A Case Study of MSI-367. Biochemistry. 2010; 49:10595–10605. [PubMed: 21062093]

42. Wang T, Li D, Lu X, Khmaladze A, Han X, Ye S, Yang P, Xu G, He N, Chen Z. Single Lipid Bilayers Constructed on Polymer Cushion Studied by Sum Frequency Generation Vibrational Spectroscopy. J. Phys. Chem C. 2011; 115:7613–7620.

43. Yang P, Ramamoorthy A, Chen Z. Membrane Orientation of MSI-78 Measured by Sum Frequency Generation Vibrational Spectroscopy. Langmuir. 2011; 27:7760–7767. [PubMed: 21595453]

44. Boughton AP, Yang P, Tesmer VM, Ding B, Tesmer JJ, Chen Z. Heterotrimeric G protein $\beta 1\gamma 2$ Subunits Change Orientation upon Complex Formation with G Protein-coupled Receptor Kinase 2 (GRK2) on a Model Membrane. Proc. Natl. Acad. Sci. U.S.A. 2011; 108:E667–E673. [PubMed: 21876134]

45. Nguyen K, Le Clair SV, Ye S, Chen Z. Orientation Determination of Protein Helical Secondary Structures Using Linear and Nonlinear Vibrational Spectroscopy. J. Phys. Chem B. 2009; 113:12169–12180. [PubMed: 19650636]

46. Nguyen KT, Le Clair S, Ye SJ, Chen Z. Molecular Interaction between Magainin 2 and Model Membranes in Situ. J. Phys. Chem. B. 2009; 113:12358–12363. [PubMed: 19728722]

47. Ding B, Chen Z. Molecular Interactions Between Cell Penetrating Peptide Pep-1 and Model Cell Membranes. J. Phys. Chem B. 2012; 116:2545–2552. [PubMed: 22292835]

48. Chen X, Wang J, Boughton AP, Kristalyn CB, Chen Z. Multiple Orientation of Melittin inside a Single Lipid Bilayer Determined by Combined Vibrational Spectroscopic Studies. J. Am. Chem. Soc. 2007; 129:1420–1427. [PubMed: 17263427]

49. Nguyen K, Soong R, Im S, Waskell L, Ramamoorthy A, Chen Z. Probing the Spontaneous Membrane Insertion of a Tail-Anchored Membrane Protein by Sum Frequency Generation Spectroscopy. J. Am. Chem. Soc. 2010; 132:15112–15115. [PubMed: 20932011]

50. Chen X, Boughton AP, Tesmer JJG, Chen Z. In Situ Investigation of Heterotrimeric G Protein $\beta\gamma$ Subunit Binding and Orientation on Membrane Bilayers. J. Am. Chem. Soc. 2007; 129:12658–12659. [PubMed: 17902674]

51. Nguyen K, King JT, Chen Z. Determination of Interfacial β-Sheet Structures in Situ. J. Phys. Chem. B. 2010; 114:8291–8300. [PubMed: 20504035]

52. Han X, Soblosky L, Slutsky M, Mello CM, Chen Z. Solvent Effect and Time-Dependent Behavior of C-Terminus Cysteine Modified Cecropin P1 Chemically Immobilized onto Polymer Surface. Langmuir. 2011; 27:7042–7051. [PubMed: 21553837]

53. Chen Z. Investigating Buried Polymer Interfaces using Sum Frequency Generation Vibrational Spectroscopy. Prog. Polym. Sci. 2010; 35:1376–1402. [PubMed: 21113334]

54. Chen X, Chen Z. SFG Studies on Interactions between Antimicrobial Peptides and Supported Lipid Bilayers. Biochim. Biophys. Acta. 2006; 1758:1257–1272. [PubMed: 16524559]

55. Chen XY, Clarke ML, Wang J, Chen Z. Sum Frequency Generation Vibrational Spectroscopy Studies on Molecular Conformation and Orientation of Biological Molecules at Interfaces. Int. J. Mod. Phys. B. 2005; 19:691–713.

56. Ye S, Nguyen K, Le Clair SV, Chen Z. In Situ Molecular Level Studies on Membrane Related Peptides and Proteins in Real Time Using Sum Frequency Generation Vibrational. J. Struct. Biol. 2009; 168:61–77. [PubMed: 19306928]

57. Wang J, Chen C, Buck SM, Chen Z. Molecular Chemical Structure on Poly(methyl methacrylate) (PMMA) Surface Studied by Sum Frequency Generation (SFG) Vibrational Spectroscopy. J. Phys. Chem. B. 2001; 105:12118–12125.

58. Wang J, Paszti Z, Even MA, Chen Z. Measuring Polymer Surface Ordering Differences in Air and in Water by Sum Frequency Generation (SFG) Vibrational Spectroscopy. J. Am. Chem. Soc. 2002; 124:7016–7023. [PubMed: 12059225]

59. Wang J, Even MA, Chen X, Schmaier AH, Waite JH, Chen Z. Detection of Amide I Signals of Interfacial Proteins in situ Using SFG. J. Am. Chem. Soc. 2003; 125:9914–9915. [PubMed: 12914441]

60. Chen X, Wang J, Sniadecki JJ, Even MA, Chen Z. Probing Alpha-helical and Beta-sheet Structures of Peptides at Solid/Liquid Interfaces with SFG. Langmuir. 2005; 21:2662–2264. [PubMed: 15779931]

61. Ye S, Liu G, Li H, Chen F, Wang X. Effect of Dehydration on the Interfacial Water Structure at a Charged Polymer Surface: Negligible $\chi(3)$ Contribution to Sum Frequency Generation Signal. Langmuir. 2012; 28:1374–1380. [PubMed: 22149290]

62. Ye S, Wei F. An Approach to Compatible Multiple Nonlinear Vibrational Spectroscopy Measurements using a Commercial Sum Frequency Generation System. Analyst. 2011; 136:2489–2494. [PubMed: 21519591]

63. Haupert LM, Simpson GJ. Chirality in Nonlinear Optics. Annu. Rev. Phys. Chem. 2009; 60:345–365. [PubMed: 19046125]

64. Simpson GJ. Molecular Origins of the Remarkable Chiral Sensitivity of Second-Order Nonlinear Optics. ChemPhysChem. 2004; 5:1301–1310. [PubMed: 15499846]

65. Moad AJ, Simpson GJ. Self-Consistent Approach for Simplifying the Molecular Interpretation of Nonlinear Optical and Multiphoton Phenomena. J. Phys. Chem A. 2005; 109:1316–1323. [PubMed: 16833446]

66. Liljeblad JFD, Bulone V, Rutland MW, Johnson CM. Supported Phospholipid Monolayers. The Molecular Structure Investigated by Vibrational Sum Frequency Spectroscopy. J. Phys. Chem C. 2011; 115:10617–10629.

67. Liljeblad JFD, Bulone V, Tyrode E, Rutland MW, Johnson CM. Phospholipid Monolayers Probed by Vibrational Sum Frequency Spectroscopy: Instability of Unsaturated Phospholipids. Biophys. J. 2010; 98:L50–L52. [PubMed: 20483309]

68. Nishida T, Johnson CM, Holman J, Osawa M, Davies PB, Ye S. Optical Sum-Frequency Emission from Langmuir-Blodgett Films of Variable Thickness: Effects of the Substrate and Polar Orientation of Fatty Acids in the Films. Phys. Rev. Lett. 2006; 96:077402/1–077402/4. [PubMed: 16606140]

69. Tong Y, Li N, Liu H, Ge A, Osawa M, Ye S. Mechanistic Studies by Sum-Frequency Generation Spectroscopy: Hydrolysis of a Supported Phospholipid Bilayer by Phospholipase A2. Angew. Chem. Int. Ed. 2010; 49:2369–2373.

70. Li G, Ye S, Morita S, Nishida T, Osawa M. Hydrogen Bonding on the Surface of Poly(2-methoxyethyl acrylate). J. Am. Chem. Soc. 2004; 126:12198–12199. [PubMed: 15453716]

71. Ye S, Osawa M. Molecular Structures on Solid Substrates Probed by Sum Frequency Generation (SFG) Vibration Spectroscopy. Chem. Lett. 2009; 38:386–391.

72. Barth C, Jakubczyk D, Kubas A, Anastassacos F, Brenner-Weiss G, Fink K, Schepers U, Brase S, Koelsch P. Interkingdom Signaling: Integration, Conformation, and Orientation of N-Acyl-l-homoserine Lactones in Supported Lipid Bilayers. Langmuir. 2012; 28:8456–8462. [PubMed: 22568488]

73. Engelhardt K, Rumpel A, Walter J, Dombrowski J, Kulozik U, Braunschweig B, Peukert W. Protein Adsorption at the Electrified Air–Water Interface: Implications on Foam Stability. Langmuir. 2012; 28:7780–7787. [PubMed: 22530646]

74. Liu J, Conboy JC. Structure of a Gel Phase Lipid Bilayer Prepared by the Langmuir–Blodgett/Langmuir-Schaefer Method Characterized by Sum-Frequency Vibrational Spectroscopy. Langmuir. 2005; 21:9091–9097. [PubMed: 16171337]

75. Liu J, Conboy JC. Phase Transition of a Single Lipid Bilayer Measured by Sum-Frequency Vibrational Spectroscopy. J. Am. Chem. Soc. 2004; 126:8894–8895. [PubMed: 15264810]

76. Anglin TC, Liu J, Conboy JC. Facile Lipid Flip-Flop in a Phospholipid Bilayer Induced by Gramicidin A Measured by Sum-Frequency Vibrational Spectroscopy. Biophys. J. 2007; 92:L01–L03. [PubMed: 17071658]

77. Anglin TC, Brown KL, Conboy JC. Phospholipid flip-flop modulated by transmembrane peptides WALP and melittin. J. Struct. Biol. 2009; 168:37–52. [PubMed: 19508895]

78. Anglin TC, Cooper MP, Li H, Chandler K, Conboy JC. Free Energy and Entropy of Activation for Phospholipid Flip-Flop in Planar Supported Lipid Bilayers. J. Phys. Chem. B. 2010; 114:1903–1914. [PubMed: 20073520]

79. Fu L, Ma G, Yan EC. In Situ Misfolding of Human Islet Amyloid Polypeptide at Interfaces Probed by Vibrational Sum Frequency Generation. J. Am. Chem. Soc. 2010; 132:5405–5412. [PubMed: 20337445]

80. Fu L, Liu J, Yan EC. Chiral Sum Frequency Generation Spectroscopy for Characterizing Protein Secondary Structures at Interfaces. J. Am. Chem. Soc. 2011; 122:8094–8097. [PubMed: 21534603]

81. Ma G, Liu DF, Allen HC. Piperidine Adsorption on Hydrated α-Alumina (0001) Surface Studied by Vibrational Sum Frequency Generation Spectroscopy. Langmuir. 2004; 20:11620–11629. [PubMed: 15595791]

82. Weidner T, Breen NF, Drobny GP, Castner DG. Amide or Amine: Determining the Origin of the 3300 cm–1 NH Mode in Protein SFG Spectra Using 15N Isotope Labels. J. Phys. Chem. B. 2009; 113:15423–15426. [PubMed: 19873996]

83. Weidner T, Samuel NT, McCrea K, Gamble LJ, Ward RS, Castner DG. Assembly and Structure of α-helical Peptide Films on Hydrophobic Fluorocarbon Surfaces. Biointerphases. 2010; 5:9–16. [PubMed: 20408730]

84. Weidner T, Breen NF, Li K, Drohny GP, Castner DG. Sum Frequency Generation and Solid-state NMR Study of the Structure, Orientation, and Dynamics of Polystyrene-adsorbed Peptides. Proc. Natl. Acad. Sci. U.S.A. 2010; 107:13288–13293. [PubMed: 20628016]
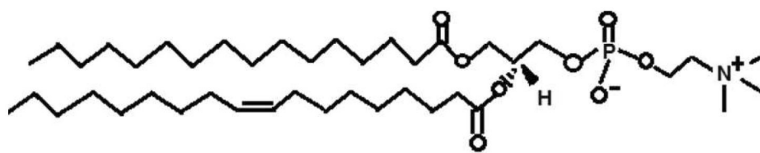
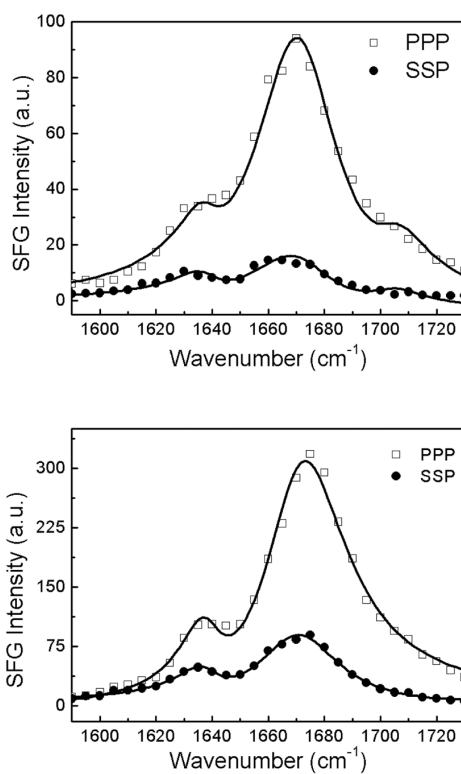**Scheme 1.**
Molecular structure of the lipid POPC:

Figure 1.
SFG ppp and ssp amide I spectra collected from a POPC/POPC bilayers in contact with a 0.84 µM (top) or 15.6 µM (bottom) alamethicin solution.
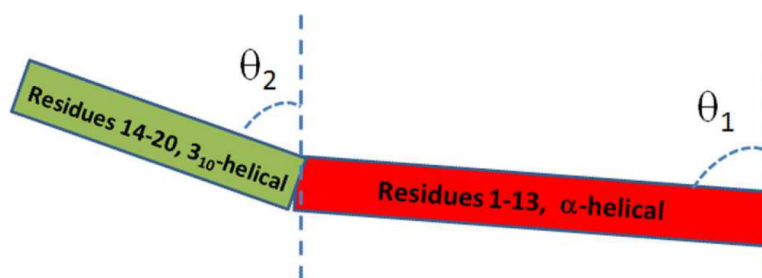
Figure 2.
The definition of the two tilt angles of alamethicin associated with a POPC/POPC bilayer.
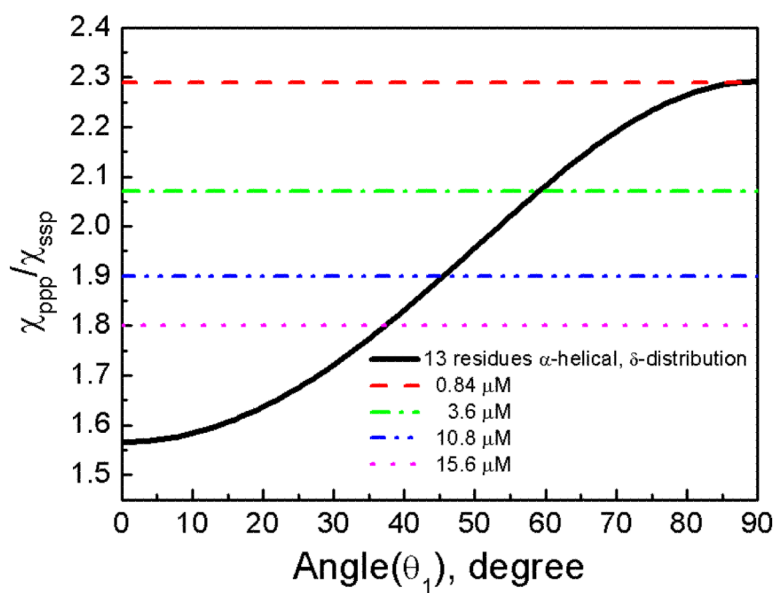
Figure 3.
Relation between the χ_{ppp}/χ_{ssp} ratio and the a-helical segment orientation angle in a POPC/POPC bilayer (assuming a delta angle distribution). The dotted lines are experimental data.
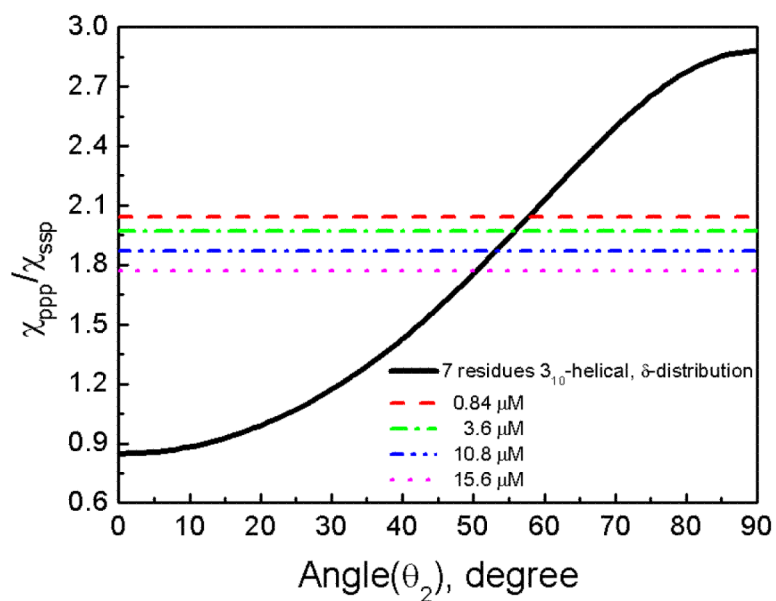
Figure 4.
Relation between the χ_{ppp}/χ_{ssp} ratio and the 3_{10}-helical structure orientation angle in a POPC/POPC bilayer (assuming a delta angle distribution). The dotted lines are experimental data.
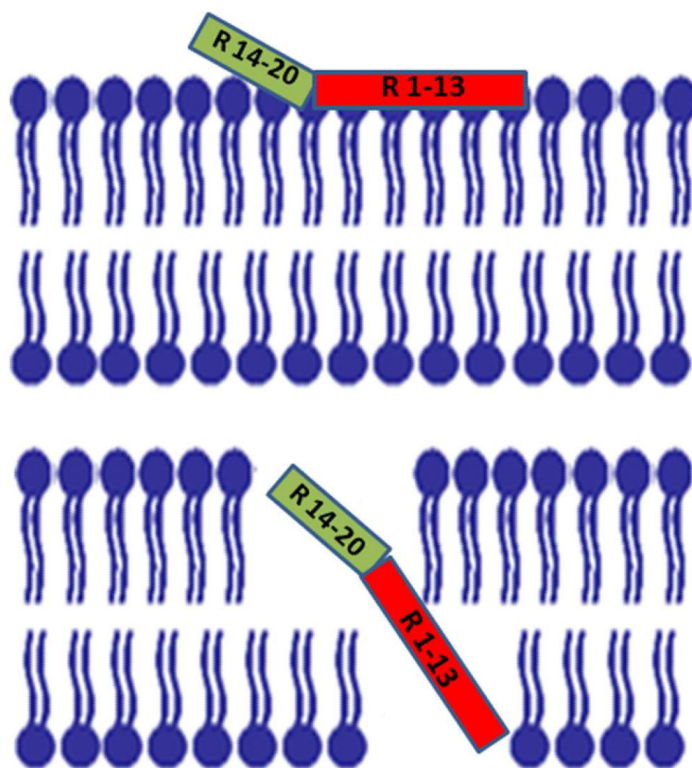
Figure 5.
Schematics showing the orientation of alamethicin in a POPC/POPC bilayer at 0.84 µM (top) or 15.6 µM (bottom) peptide solution concentration.
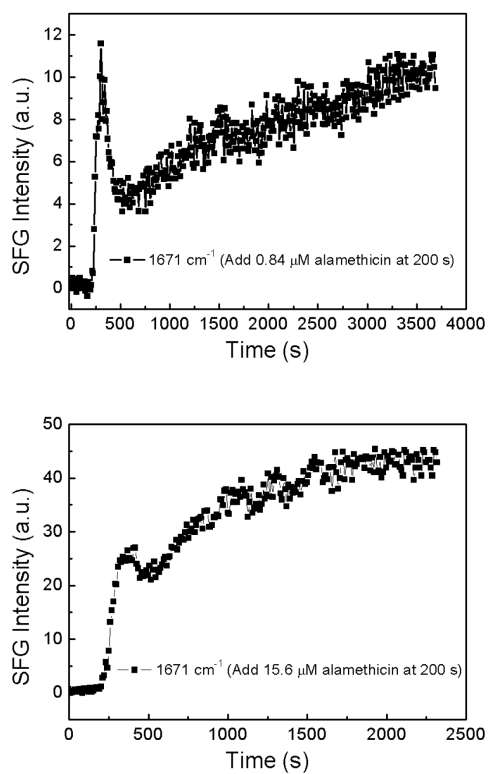
Figure 6.
Time dependent ssp SFG spectral intensity monitored at 1671 cm^{-1} (from αhelical) in POPC/POPC bilayer with 0.84 μM (top) and 15.6 μM (bottom) peptide solution concentrations. The alamethicin solution was injected at 200 s.

Table 1

Fitting parameters and fitting errors for SFG spectra shown in Figure 1. The fitting errors are included in parentheses. χ_{NR} is the nonresonant background, A is signal strength, ω is resonant frequency and Γ is damping coefficient. More details about the SFG peak fitting method can be found in reference 46.

		0.84 µM alamethicin solution			15.6 µM alamethicin solution		
		ssp	ppp	$\dfrac{(A/\Gamma)_{ppp}}{(A/\Gamma)_{ssp}}$	ssp	ppp	$\dfrac{(A/\Gamma)_{ppp}}{(A/\Gamma)_{ssp}}$
χ_{NR}		−0.80	−0.43		−0.65	1.47	
Peak 1	A	11.4(1.7)	23.3(2.3)		26.2(1.7)	46.3(3.1)	
	$\omega(cm^{-1})$	1638	1638	2.04	1638	1638	1.77
	$\Gamma(cm^{-1})$	9.0	9.0		9.0	9.0	
Peak 2	A	69.0(1.8)	158.0(1.8)		169.3(1.7)	304.8(2.7)	
	$\omega(cm^{-1})$	1671	1671	2.29	1671	1671	1.80
	$\Gamma(cm^{-1})$	18.0	18.0		18.0	18.0	
Peak 3	A	17.8 (2.3)	23.1(3.3)		0(/)	0(/)	
	$\omega(cm^{-1})$	1705	1705	1.30	1705	1705	/
	$\Gamma(cm^{-1})$	12.0	12.0		12.0	12.0	

Table 2

Orientation angles deduced from SFG data for α-helical segment (θ_1) and 3_{10}-helical segment (θ_2) in alamethicin associated with the POPC/POPC bilayer with different peptide solution concentrations.

Solution concentrations	θ_1, α-helix	θ_2, 3_{10}-helix
0.84 μM	88°	58°
3.6 μM	59°	56°
10.8 μM	46°	53°
15.6 μM	37°	50°